

**Valparaiso University**

---

**From the Selected Works of Rob Swanson**

---

October, 2009

# Is a Long-Chain Fatty Acid omega-Hydroxylase Essential for Sporopollenin Synthesis in Pollen of Arabidopsis. *Plant Physiology*

Rob Swanson, *Valparaiso University*

Anna A Dobritsa

Jay Shrestha

Marc Morant

Franck Pinot, et al.



Available at: [https://works.bepress.com/rob\\_swanson/9/](https://works.bepress.com/rob_swanson/9/)

# CYP704B1 Is a Long-Chain Fatty Acid $\omega$ -Hydroxylase Essential for Sporopollenin Synthesis in Pollen of *Arabidopsis*<sup>1[W][OA]</sup>

Anna A. Dobritsa<sup>2\*</sup>, Jay Shrestha<sup>2</sup>, Marc Morant<sup>3</sup>, Franck Pinot, Michiyo Matsuno, Robert Swanson, Birger Lindberg Møller, and Daphne Preuss<sup>4</sup>

Department of Molecular Genetics and Cell Biology, University of Chicago, Chicago, Illinois 60637 (A.A.D., J.S., D.P.); Plant Biochemistry Laboratory, Department of Plant Biology and Biotechnology, Faculty of Life Sciences and VKR Research Centre "Pro-Active Plants," University of Copenhagen, DK-1871 Frederiksberg C, Copenhagen, Denmark (M.M., B.L.M.); Institut de Biologie Moléculaire des Plantes, CNRS UPR2357-Université de Strasbourg, Département Réseau Métabolique, F-67083 Strasbourg cedex, France (F.P., M.M.); and Department of Biology, Valparaiso University, Valparaiso, Indiana 46383 (R.S.)

Sporopollenin is the major component of the outer pollen wall (exine). Fatty acid derivatives and phenolics are thought to be its monomeric building blocks, but the precise structure, biosynthetic route, and genetics of sporopollenin are poorly understood. Based on a phenotypic mutant screen in *Arabidopsis* (*Arabidopsis thaliana*), we identified a cytochrome P450, designated CYP704B1, as being essential for exine development. CYP704B1 is expressed in the developing anthers. Mutations in CYP704B1 result in impaired pollen walls that lack a normal exine layer and exhibit a characteristic striped surface, termed *zebra* phenotype. Heterologous expression of CYP704B1 in yeast cells demonstrated that it catalyzes  $\omega$ -hydroxylation of long-chain fatty acids, implicating these molecules in sporopollenin synthesis. Recently, an anther-specific cytochrome P450, denoted CYP703A2, that catalyzes in-chain hydroxylation of lauric acid was also shown to be involved in sporopollenin synthesis. This shows that different classes of hydroxylated fatty acids serve as essential compounds for sporopollenin formation. The genetic relationships between CYP704B1, CYP703A2, and another exine gene, *MALE STERILITY2*, which encodes a fatty acyl reductase, were explored. Mutations in all three genes resulted in pollen with remarkably similar *zebra* phenotypes, distinct from those of other known exine mutants. The double and triple mutant combinations did not result in the appearance of novel phenotypes or enhancement of single mutant phenotypes. This implies that each of the three genes is required to provide an indispensable subset of fatty acid-derived components within the sporopollenin biosynthesis framework.

The biopolymer sporopollenin is the major component of the outer walls in pollen and spores (exines). It is highly resistant to nonoxidative physical, chemical, and biological treatments and is insoluble in both aqueous and organic solvents. While the stability and resistance of sporopollenin account for the preserva-

tion of ancient pollen grains for millions of years with nearly full retention of morphology (Doyle and Hickey, 1976; Friis et al., 2001), these same qualities make it extremely difficult to study the chemical structure of sporopollenin. Thus, although the first studies on the composition of sporopollenin were reported in 1928 (Zetsche and Huggler, 1928), the exact structure of sporopollenin remains unresolved. At present, it is thought that sporopollenin is a complex polymer primarily made of a mixture of fatty acids and phenolic compounds (Guilford et al., 1988; Wiermann et al., 2001).

Fatty acids were first implicated as sporopollenin components when ozonolysis of *Lycopodium clavatum* and *Pinus sylvestris* exine yielded significant amounts of straight- and branched-chain monocarboxylic acids, characteristic fatty acid breakdown products (Shaw and Yeadon, 1966). More recently, improved purification and degradation techniques coupled with analytical methods, such as solid-state <sup>13</sup>C-NMR spectroscopy, Fourier transform infrared spectroscopy, and <sup>1</sup>H-NMR, have shown that sporopollenin is made up of polyhydroxylated unbranched aliphatic units and also contains small amounts of oxygenated aromatic rings and phenylpropanoids (Guilford et al., 1988; Ahlers et al.,

<sup>1</sup> This work was supported by the National Science Foundation Arabidopsis 2010 project (grant no. MCB-0520283 to D.P.), by a Danish National Research Foundation grant to the Center of Molecular Plant Physiology, and by a Villum Kann Rasmussen Foundation grant to the VKR Research Centre "Pro-Active Plants" (to B.L.M.).

<sup>2</sup> These authors contributed equally to the article.

<sup>3</sup> Present address: Department of Microbial Discovery, Novozymes A/S, 2880 Bagsvaerd, Denmark.

<sup>4</sup> Present address: Chromatin, Inc., Chicago, IL 60616.

\* Corresponding author; e-mail [dobritsa@uchicago.edu](mailto:dobritsa@uchicago.edu).

The author responsible for distribution of materials integral to the findings presented in this article in accordance with the policy described in the Instructions for Authors ([www.plantphysiol.org](http://www.plantphysiol.org)) is: Anna A. Dobritsa ([dobritsa@uchicago.edu](mailto:dobritsa@uchicago.edu)).

[W] The online version of this article contains Web-only data.

[OA] Open Access articles can be viewed online without a subscription.

[www.plantphysiol.org/cgi/doi/10.1104/pp.109.144469](http://www.plantphysiol.org/cgi/doi/10.1104/pp.109.144469)

1999; Domínguez et al., 1999; Bubert et al., 2002). Biochemical studies using thiocarbamate herbicide inhibition of the chain-elongating steps in the synthesis of long-chain fatty acids and radioactive tracer experiments provided further evidence that lipid metabolism is involved in the biosynthesis of sporopollenin (Wilwesmeier and Wiermann, 1995; Meuter-Gerhards et al., 1999).

Relatively little is known about the genetic network that determines sporopollenin synthesis. However, several *Arabidopsis* (*Arabidopsis thaliana*) genes implicated in exine biosynthesis encode proteins with sequence homology to enzymes that are involved in fatty acid metabolism. Mutations in *MALE STERILITY2* (*MS2*) eliminate exine and affect a protein with sequence similarity to fatty acyl reductases; the predicted inability of *ms2* plants to reduce pollen wall fatty acids to the corresponding alcohols suggests that this reaction is a key step in sporopollenin synthesis (Aarts et al., 1997). The *FACELESS POLLEN1* (*FLP1*) gene, whose loss causes the *flp1* exine defect, encodes a protein similar to those involved in wax synthesis (Ariizumi et al., 2003). The *no exine formation1* (*nef1*) mutant accumulates reduced levels of lipids, and the NEF1 protein was suggested to be involved in either lipid transport or the maintenance of plastid membrane integrity, including those plastids in the secretory tapetum of anthers, where many of the sporopollenin components are synthesized (Ariizumi et al., 2004). The *dex2* mutant has mutations in the evolutionarily conserved anther-specific cytochrome P450, CYP703A2 (Morant et al., 2007), which catalyzes in-chain hydroxylation of saturated medium-chain fatty acids, with lauric acid (C12:0) as a preferred substrate (Morant et al., 2007). A recently described gene, *ACOS5*, encodes a fatty acyl-CoA synthetase that has in vitro preference for medium-chain fatty acids (de Azevedo Souza et al., 2009). Mutations in all of these genes compromise exine formation.

Here, we describe an evolutionarily conserved cytochrome P450, CYP704B1, and demonstrate that this gene is essential for exine biosynthesis and plays a role different from that of CYP703A2. Heterologously expressed CYP704B1 catalyzed  $\omega$ -hydroxylation of several saturated and unsaturated C14-C18 fatty acids. These results suggest the possibility that  $\omega$ -hydroxylated fatty acids produced by CYP704B1, together with in-chain hydroxylated lauric acids provided by the action of CYP703A2, may serve as key monomeric aliphatic building blocks in sporopollenin formation. Analyses of the genetic relationships between *CYP704B1*, *MS2*, and *CYP703A2* suggest that all three genes are involved in the same pathway within the sporopollenin biosynthesis framework.

## RESULTS

### *zebra* Mutants Have Impaired Pollen Wall Architecture

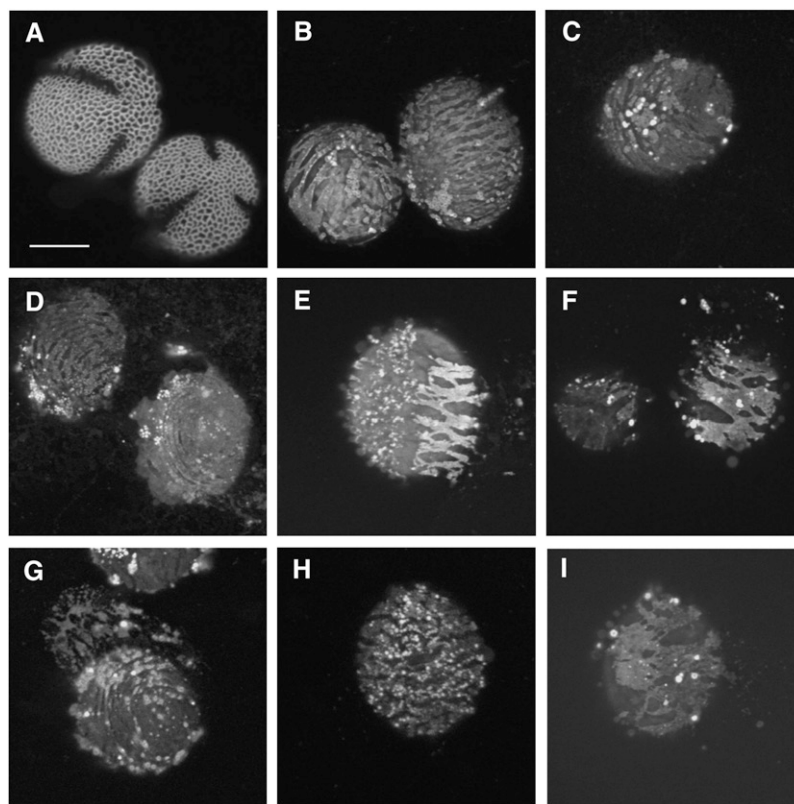
We performed a large-scale genetic screen in *Arabidopsis* aimed at identification of mutants with defects

in pollen exine production. In this screen, we recovered, among others, a particular phenotypic class of mutants with anthers that contained pollen that was not easily shed and appeared glossy with a dissection microscope. Close examination by laser scanning confocal microscopy (LSCM) of auramine O-stained pollen grains revealed that the mutant pollen lacked normal exine (Fig. 1). The exine was replaced with a thin layer of a material that did not stain well with auramine O (Fig. 1, B–I). A rare and irregular distribution of aggregates that stained densely with auramine O was also present. A typical characteristic of the surface was the presence of dark, non-auramine O-positive stripes (Fig. 1, B–I). Accordingly, we refer to this mutant class as having a *zebra* pollen phenotype. Seven mutant lines that had *zebra* phenotypes were discovered through a forward genetics screen, and one line was identified through a reverse genetics approach.

### *zebra* Mutants Form Two Complementation Groups, One of Which Maps to the At1g69500 Gene

In order to establish complementation groups for the eight mutant lines with *zebra* pollen phenotypes, we performed pair-wise complementation crosses. These crosses placed the mutants in two complementation groups, with line 135-2-3 being the sole member of one group and the rest of the lines belonging to a different group. The latter complementation group included a T-DNA insertion into the gene At1g69500 (SAIL\_1149\_B03); this line was tested because the disrupted gene had a predicted anther-specific expression pattern. To confirm that the *zebra* pollen phenotype is caused by the insertion into At1g69500, we rescued the mutant phenotype with the wild-type copy of the gene, which restored a reticulate exine pattern (Supplemental Fig. S1). To determine if other members of this complementation group also had defects in At1g69500, we PCR amplified and sequenced the corresponding gene. We found that all of the mutant lines from this complementation group had polymorphisms within the open reading frame of At1g69500. Several of the mutants had point mutations in At1g69500. Lines 28-3-1 and 131-3-1 had a single nucleotide deletion of T in codon 46, resulting in a frameshift mutation, soon followed by a stop codon. Lines 119-1-1 and 155-4-1 exhibited an A-to-G substitution, resulting in a nonconservative Lys-401 → Glu change at the amino acid level, while line 174-154-2 contained an A-to-T substitution that resulted in the replacement of Arg-469 with Trp. Recoveries of point mutations in other genes through T-DNA screens have been previously described (Dieterle et al., 2001; Takeda et al., 2004; Marrocco et al., 2006). Lines carrying identical mutations were discovered in different pools of mutagenized SALK lines, yet we cannot exclude the possibility that they may be related. In line 37-2-3, unlike in the other lines, we were unable to PCR amplify the entire gene using a pair of primers

**Figure 1.** *zebra* mutants have defective exine architecture. Confocal images of exine surface from the wild-type (A) and mutant (B–I) pollen grains that exhibit *zebra* phenotypes. Pollen was stained with the fluorescent dye auramine O and visualized using fluorescein isothiocyanate settings. Pollen from the following lines are shown: SAIL\_1149\_B03 (B), 28-3-1 (C), 37-2-3 (D), 119-1-1 (E), 131-3-1 (F), 155-4-1 (G), 174-154-2 (H), and 135-2-3 (I). All images are to the same magnification. Bar = 10  $\mu$ m.



that spanned this region. Upon close analysis, we found that a region of approximately 440 nucleotides that contained the fourth out of the six exons could not be amplified by flanking primers or primers hybridizing within this region. These data indicate that a genomic rearrangement had likely occurred, which was not further investigated. Bulked segregant analysis (Michelmore et al., 1991) performed on two of these *zebra* lines (28-3-1 and 37-2-3) confirmed that the phenotypes were linked to the bottom of chromosome 1 (markers NGA111 and NGA692) in the general vicinity of At1g69500. Taken together, these results demonstrate that we identified five distinct mutant alleles of At1g69500 (Fig. 2A). The expression of At1g69500 mRNA in the T-DNA insertion mutant was examined by reverse transcription (RT)-PCR. The At1g69500 transcript was detected in the mRNA isolated from the wild-type control but not in the mRNA from the T-DNA insertion line (Fig. 2B). This mutant was used for all further experiments.

#### Pollen from At1g69500 Mutants Lacks Exine

The exine pattern in At1g69500 mutants was further analyzed using scanning electron microscopy (SEM). While wild-type pollen exhibited characteristic reticulate ornamentation on its surface, pollen from the At1g69500 T-DNA insertion line showed a complete lack of any reticulate exine pattern (Fig. 3, A–D). When SEM analysis was conducted without prior fixation, we observed that the mutant pollen collapsed, while

wild-type pollen resisted the vacuum applied during gold coating and SEM (Fig. 3, A and B). This indicated that *zebra* mutants lacked the structural and physical support provided by the exine layer. Analysis of wild-type and mutant pollen using transmission electron microscopy showed dramatic differences in the structure of the pollen walls. While the baculae, tectum, and pollen coat were readily observed on the wild-type pollen surface (Fig. 3E), these structures were completely missing from the At1g69500 mutant pollen wall, replaced by a very thin layer of an electron-dense material (Fig. 3, F and G). We did not notice significant changes in the intine layer of At1g69500 mutants.

Some, but not all, exine mutants are sensitive to acetolysis (Aarts et al., 1997; Ariizumi et al., 2003; A.A. Dobritsa, unpublished data), an oxidative procedure used for preparation of exine samples that involves incubation of pollen in a mixture of acetic anhydride and sulfuric acid (Erdtman, 1960). In the absence of a normal exine layer, the At1g69500 mutants became sensitive to acetolysis. While mock-treated wild-type and At1g69500 mutant pollen grains maintained a similar appearance (Fig. 3, I and J), dramatic differences between the wild-type and mutant pollen were observed following acetolysis (Fig. 3, K and L). The At1g69500 mutant grains underwent rapid lysis (Fig. 3L), while wild-type pollen grains remained intact and their exine features were enhanced after interaction with acetolysis mixture (Fig. 3K).

Surprisingly, despite such dramatic alterations in the pollen wall structure, none of the At1g69500 mu-

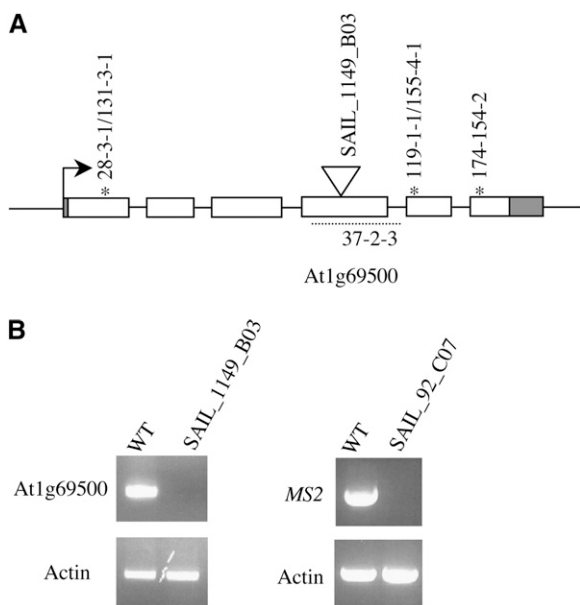


**Figure 2.** One *zebra* complementation group maps to the At1g69500 gene. A, The exon-intron map of the At1g69500 gene. White boxes represent coding regions, and the gray box represents the untranslated region. Positions of the identified point mutations are indicated by asterisks, and the position of the T-DNA insertion is indicated by a triangle. The dashed line indicates the region that could not be PCR amplified in line 37-2-3; however, the exact nature of this mutation was not defined. B, At1g69500 and *MS2* gene expression in stage 9 to 10 buds from At1g69500 and *ms2* T-DNA mutants was assessed with RT-PCR. Line SAIL\_1149\_B03 was used for the At1g69500 mutant, and SAIL\_92\_C07 was used for *ms2*. Actin1 was used as a control. WT, Wild type.

tants had apparent changes in fertility under the growth conditions used in this study, with all the alleles producing long, well-developed siliques. The T-DNA insertion line produced  $50 \pm 6$  seeds per silique (mean  $\pm$  SD;  $n = 10$  siliques) versus  $55 \pm 5$  seeds per silique for the wild type ( $n = 10$  siliques). Mature pollen from mutant lines contained two generative cells and a single vegetative nucleus (Supplemental Fig. S2), indicating that meiotic and mitotic divisions occurred normally.

#### At1g69500 Has an Anther-Specific Expression Pattern

A search of the publicly available expression databases, such as Genevestigator (Zimmermann et al., 2004; <https://www.genevestigator.ethz.ch/>) and Massively Parallel Signature Sequencing (Meyers et al., 2004; <http://mpss.udel.edu/at/>), to evaluate tissue expression patterns of At1g69500 suggested that this gene is specifically expressed in young anthers and in flower buds of stages 9 and 10. Transcripts were absent in flower buds from the *ap3* and *ag* mutants that lack stamens. Additionally, a search for coexpressed genes using the Arabidopsis trans-factor and cis-element prediction database ATTED-II (Obayashi et al., 2007;

<http://www.atted.bio.titech.ac.jp/>) and the BAR Expression Angler (Toufighi et al., 2005; [http://bbc.botany.utoronto.ca/ntools/cgi-bin/ntools\\_expression\\_angler.cgi](http://bbc.botany.utoronto.ca/ntools/cgi-bin/ntools_expression_angler.cgi)) demonstrated that At1g69500 had the highest correlation for coexpression with *MS2* and *CYP703A2*, two anther-specific genes known to be involved in exine development (Aarts et al., 1997; Morant et al., 2007). This likely suggests related functions of these three proteins in exine biosynthesis. Furthermore, searches in the EST databases for At1g69500 orthologs revealed the presence of the corresponding transcripts in anther or flower bud cDNA libraries from the eudicots *Brassica* (accession nos. EX048874, EX048869, and EV141925) and *Aquilegia* (DT748122 and DT767118), the monocots maize (*Zea mays*; AAK52956), sorghum (*Sorghum bicolor*; Albertsen et al., 2006), and *Aegilops speltoides* (BQ840694), and the microsporophyll cDNA library of the gymnosperm *Ginkgo biloba* (EX932454 and EX934753).

To confirm the anther-specific expression of At1g69500, we performed RT-PCR using At1g69500-specific primers. The At1g69500 transcript was readily detectable in buds and flowers but not in roots, rosette leaves, stems, cauline leaves, or green siliques (Fig. 4A). In addition, we transformed wild-type plants with GUS under the control of the At1g69500 promoter. In the resulting T1 plants, GUS staining was observed only in anthers of developing buds: GUS expression was first noticeable in stage 9 buds, peaked during stages 9 to 11, and faded during stage 12 (Fig. 4, B–I).

#### At1g69500 Encodes CYP704B1 and Catalyzes $\omega$ -Hydroxylation of Long-Chain Fatty Acids

At1g69500 encodes a predicted cytochrome P450, CYP704B1. Cytochromes P450 form a superfamily of diverse enzymes that catalyze a large variety of reactions, usually based on activation of molecular oxygen with insertion of one of its atoms in a substrate and reduction of the other to form water (Werck-Reichhart et al., 2002; Morant et al., 2003). Several motifs important for the P450 functions (Werck-Reichhart et al., 2002; Morant et al., 2003) can be identified in its primary structure. First, the protein has a heme-binding domain (FQAGPRICLG) containing the heme-binding consensus sequence FxxGxRxCxG in the C terminus. The mutant line 174-154-2 carries a mutation in the gene region encoding the heme-binding domain, resulting in replacement of the Arg residue by a Trp residue. Second, the protein contains a Thr-containing binding pocket for molecular oxygen required in catalysis (AGRDTT) that obeys the consensus (A/G)Gx(D/E)T(T/S). Phylogenetic analysis of cytochromes P450 places CYP704B1 into the CYP86 clan (Werck-Reichhart et al., 2002; Nelson, 2006), along with members of the CYP86, CYP94, and CYP96 families (Supplemental Fig. S3). Several members of the CYP86 and CYP94 families from this clan have been functionally defined as fatty acid  $\omega$ -hydroxylases (Benveniste et al., 1998, 2006; Tijet et al., 1998; Pinot et al., 1999; Wellesen et al., 2001; Duan and Schuler, 2005; Kandel et al.,

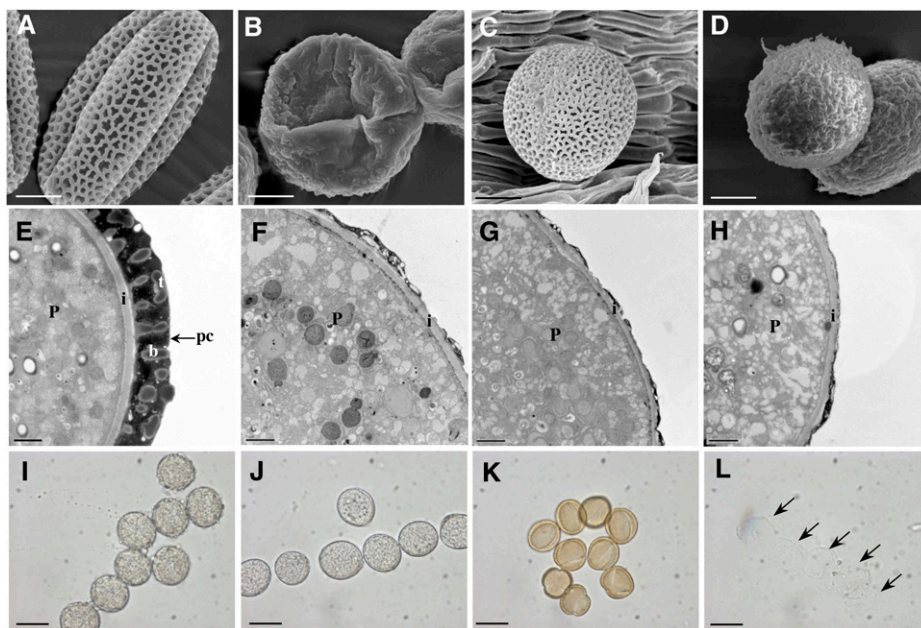


**Figure 3.** *zebra* mutants have severe defects in exine structure. A to D, Scanning electron micrographs of the surface structure of pollen grains from the wild type (A and C) and the At1g69500 mutant (allele SAIL\_1149\_B03; B and D). Samples were prepared without fixation (A and B) or with fixation (C and D). Bars = 5  $\mu\text{m}$ . E to H, Transmission electron micrographs of pollen grain sections from the wild type (E) and *zebra* mutants At1g69500 allele SAIL\_1149\_B03 (F), At1g69500 allele 119-1-1 (G), and *ms2* allele 135-2-3 (H). Bars = 1  $\mu\text{m}$ . b, Baculae; i, intine; P, pollen grain cytoplasm; pc, pollen coat; t, tectum. I and J, *zebra* mutants are sensitive to acetolysis. Wild-type (I) and At1g69500 allele SAIL\_1149\_B03 (J) pollen grains mock treated with 50 mM Tris-HCl, pH 7.5, have similar morphology. K, Wild-type pollen grains treated with the acetolysis mixture remain intact. L, At1g69500 mutant pollen is completely lysed after the acetolysis treatment. Arrows point to the remnants of five pollen grains. Bars = 20  $\mu\text{m}$ .

2006). Of particular interest is the fact that some of these fatty acid  $\omega$ -hydroxylases (CYP86A1 [Li et al., 2007; Höfer et al., 2008], CYP86A2 [Xiao et al., 2004; Molina et al., 2008], CYP86A8 [Wellesen et al., 2001], CYP86B1 [Compagnon et al., 2009], and CYP94A1 [Tijet et al., 1998; Pinot et al., 1999]) have been implicated in the production of fatty acid-derived monomers for cutin and suberin, two major lipid polymers of plants (Kollatukudy, 1981; Pollard et al., 2008). Existence of structural as well as functional similarity between sporopollenin and these two polyesters has been previously suggested (Shulze Osthoff and Wiermann, 1987; Scott, 1994).

In order to characterize the catalytic function of CYP704B1, its cDNA was cloned and expressed in yeast WAT11 cells that contained a NADPH P450 oxidoreductase capable of efficient electron transport and were optimized for the expression of plant P450s (Pompon et al., 1996). Yeast microsomes were isolated, and CYP704B1 expression level and folding state were determined by measuring the absorption of the reduced complex between P450 and carbon monoxide (Omura and Sato, 1964). Microsomes were found to contain between 0.44 and 0.74  $\mu\text{M}$  of active cytochrome P450.

Because CYP704B1 is highly coexpressed with CYP703A2, a cytochrome P450 involved in exine production that catalyzes in-chain hydroxylation of lauric

acid (C12:0; Morant et al., 2007), we first tested the ability of CYP704B1-containing and NADPH cytochrome P450 oxidoreductase-containing microsomes to metabolize this substrate. No detectable derivatives of lauric acid were observed (Fig. 5). To check whether CYP704B1 was able to use hydroxylated products formed by CYP703A2 as substrates, we coincubated CYP703A2 and CYP704B1 with lauric acid and found that hydroxy lauric acids produced by CYP703A2 were not metabolized by CYP704B1. However, regardless of the substrates tested, three major novel compounds were always observed following incubation with CYP704B1-containing microsomes (Fig. 5). The formation of these compounds was strictly dependent on the presence of NADPH (data not shown), and microsomes isolated from the WAT11 cells transformed with an empty vector did not catalyze the formation of these compounds (Fig. 5, top). This showed that the accumulated products were indeed produced by CYP704B1 using an endogenous substrate present in the microsomes. Analyses of masses and fragmentation patterns by liquid chromatography-mass spectrometry (LC-MS) identified these products as the hydroxylated palmitoleic acid (C16:1), palmitic acid (C16:0), and oleic acid (C18:1; Supplemental Fig. S4). The three fatty acid substrates from which these hydroxylated products are formed are known to be

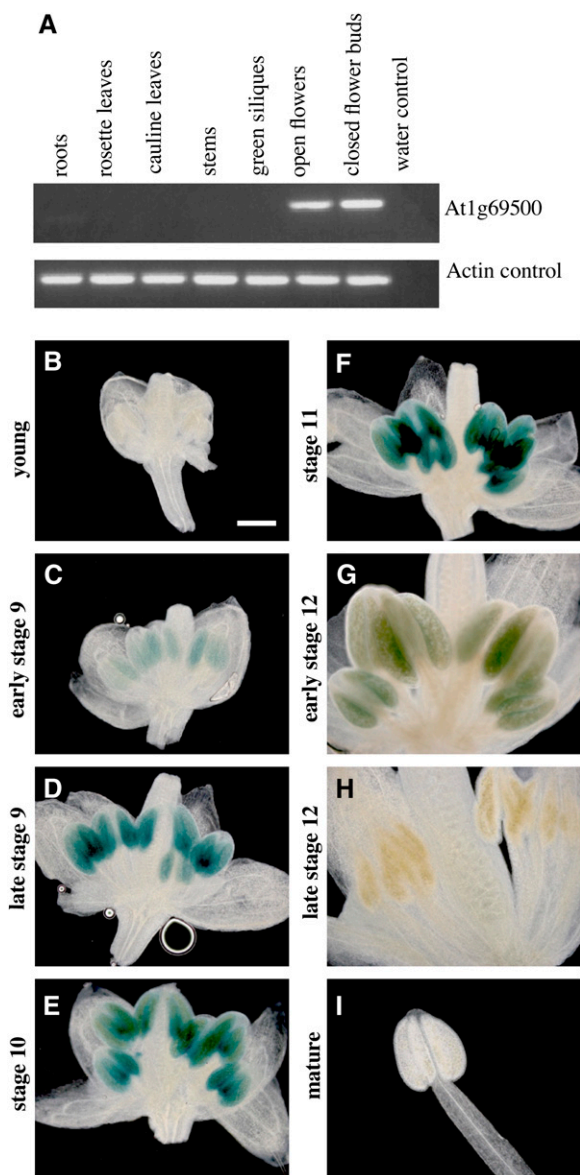


**Figure 4.** At1g69500 is expressed in the developing anthers. A, RT-PCR analysis shows flower-specific expression of At1g69500. Different tissues were collected from flowering wild-type plants and analyzed for the presence of At1g69500 transcript. Primers were designed to exclude the amplification of genomic DNA. *Actin1* was used as a control gene. B to I, The *At1g69500pr::GUS* promoter fusion construct is expressed in anthers. Expression starts in buds of stage 9 (C), is most prominent at stages 9 to 11 (D–F), and fades during stage 12 (G and H). No expression is visible before stage 9 (B) and during or after late stage 12 (H and I). All images are to the same magnification. Bar = 200  $\mu\text{m}$ .

present in the microsomal fractions from yeast grown on Glc (Tuller et al., 1999). The relative amounts of the three hydroxylated compounds formed fit with the ratio of the parent fatty acids (44% C16:1, 21% C16:0, and 28% C18:1 of total fatty acids) in the yeast microsomal fraction reported by Tuller et al. (1999).

In order to further study the substrate specificity and activity of CYP704B1, saturated and unsaturated

radioactively labeled fatty acids with chain lengths ranging from C12 to C18 were incubated at a concentration of 100  $\mu\text{M}$  with microsomes from CYP704B1-expressing yeast in the presence or absence of NADPH. Product formation was analyzed by thin-layer chromatography (TLC). Except for lauric acid (C12:0), all compounds were metabolized in the presence of NADPH, including palmitic (C16:0), oleic

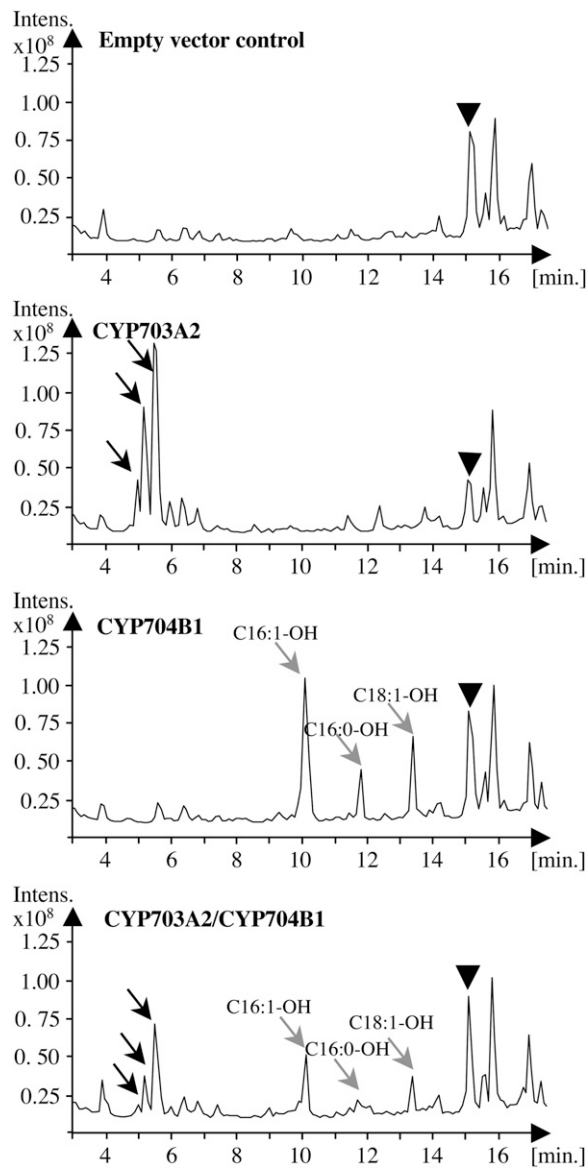


**Figure 5.** CYP704B1 metabolizes long-chain fatty acids present in yeast. Microsomes obtained from yeast transformed with an empty vector (control) and from yeast expressing CYP703A2, CYP704B1, or CYP703A2/CYP704B1 were incubated with lauric acid (10 nmol) in the presence of NADPH. Metabolites were analyzed by LC-MS. CYP703A2-expressing microsomes produced three in-chain monohydroxylated lauric acids (black arrows). Three novel peaks (C16:1-OH, C16:0-OH, and C18:1-OH; gray arrows) unrelated to lauric acid were produced by the CYP704B1-expressing microsomes. The elution position of the substrate (lauric acid) is shown by black triangles.

(C18:1), linoleic (C18:2), linolenic (C18:3), and 9,10-epoxystearic acid (epox C18) acids (Fig. 6). A single metabolite, which was produced in the presence of NADPH from palmitic acid, was purified, derivatized, and analyzed by gas chromatography-MS. Its fragmentation pattern was identical to that of the authentic derivatized commercially available 16-hydroxypalmitic acid (see "Materials and Methods"), confirming the catalytic function of CYP704B1 as an  $\omega$ -hydroxylase. Because the substrates of CYP704B1 were already present as endogenous components in the yeast microsomes, it has not been possible to calculate precise values of  $K_m$  and  $V_{max}$  for the enzyme. The precise nature of the physiological substrates of fatty acid hydroxylases in planta remains to be established. They could be free fatty acids as well as fatty acids bound to CoA or glycerol. This makes the comparison of enzymes characterized from different plants difficult. Nevertheless, the level of activity measured with CYP704B1 is similar to the activities of previously described fatty acid hydroxylases expressed using the same heterologous system and assayed using the same experimental procedure (Tijet et al., 1998; Kandel et al., 2005, 2007). It is to be noted, however, that contrary to the fatty acid hydroxylases CYP94A1 from *Vicia sativa*, CYP709C1 from wheat (*Triticum aestivum*), and CYP94C1 from Arabidopsis (Pinot et al., 1999; Kandel et al., 2005, 2007), CYP704B1 does not metabolize 9,10-epoxystearic acid with a much higher efficiency than other fatty acids tested.

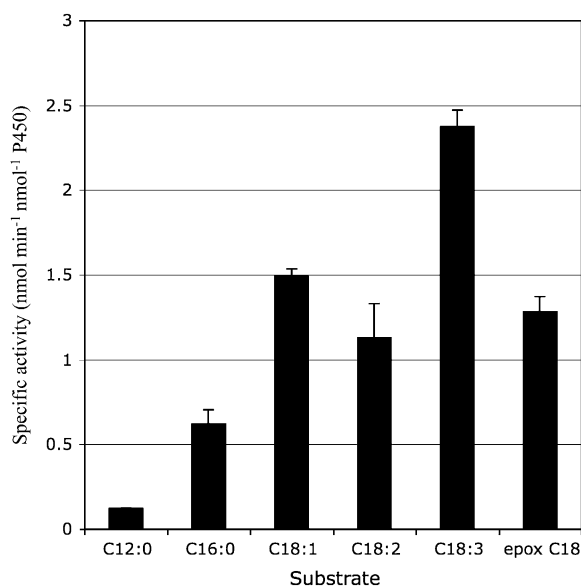


**Figure 6.** CYP704B1 metabolizes long-chain fatty acids. Microsomes were incubated with 100  $\mu$ M radioactive substrates (C12:0, lauric acid; C16:0, palmitic acid; C18:1, oleic acid; C18:2, linoleic acid; C18:3, linolenic acid; epox C18, 9,10-epoxystearic acid) in the absence or presence of NADPH, and product formation was monitored by TLC. The signal generated in the absence of NADPH was subtracted from the signal generated in the presence of NADPH. All values are means  $\pm$  SD of experiments performed in triplicate.

Phenolic compounds are also expected to act as building blocks for sporopollenin. Accordingly, we analyzed the ability of CYP704B1 to hydroxylate a number of common phenolics (cinnamate, *p*-coumarate, ferulate, sinapate, and *p*-coumaroyl shikimate) that serve as important precursors for different types of phenylpropanoids. None of these compounds was metabolized by CYP704B1 in the presence of NADPH (Fig. 7). Two cytochrome P450s (CYP73A5 and CYP98A3), which are known to have hydroxylase activity toward cinnamate and *p*-coumaroyl shikimate (Urban et al., 1997; Schoch et al., 2001), were used as positive controls.

### A Second *zebra* Complementation Group Is in the *MS2* Gene

Bulked segregant analysis of the *zebra* line 135-2-3 that complemented the phenotypes of the *cyp704b1* mutants mapped the defect to the top of chromosome 3 (markers NGA162 and GAPAB). *MS2*, a gene previously implicated in exine production and encoding a fatty acyl reductase (Aarts et al., 1997; Doan et al., 2009), resides within the same chromosomal area. Sequencing of the *MS2* gene from line 135-2-3 revealed that it had a 42-nucleotide in-frame deletion resulting in the removal of 14 amino acids (amino acids 498–511). The *ms2* transposon-induced alleles described by Aarts et al. (1993, 1997) are male sterile and produce almost no pollen. However, two T-DNA insertions in the *MS2* gene (SAIL\_92\_C07 and SAIL\_75\_E01) became available recently as part of the SAIL collection (Sessions et al., 2002). We confirmed the positions of the T-DNA insertions in these lines by genotyping and checked the phenotypes of these mutants. We found that, similar to our observations on line 135-2-3, they produced a lot of pollen and were fertile. Their pollen appeared glossy and adhered tightly to anthers, as also observed with 135-2-3 phenotypes. When stained with auramine O and examined by LSCM, SAIL\_92\_C07 and SAIL\_75\_E01 pollen was found to have the characteristic *zebra* appearance (Fig. 8, A and B). *MS2* mRNA expression in the SAIL\_92\_C07 T-DNA line was analyzed with RT-PCR. The *MS2* transcript was detected in stage 9 to 10 buds isolated from the wild-type plants but not in the SAIL\_92\_C07 plants (Fig. 2B). We performed complementation crosses between 135-2-3 and SAIL\_92\_C07 or SAIL\_75\_E01 and found that none of these lines complemented each other. This strongly suggested that 135-2-3 was a novel allele of the *MS2* gene.

Detailed examination of the exine structure in line 135-2-3 using transmission electron microscopy demonstrated a phenotype very similar to that of the *cyp704b1* mutants: baculae and tectum structures were absent and replaced by a very thin layer of a dark material (Fig. 3H).

Given that the mutants in *CYP704B1* and *MS2* have identical pollen phenotypes and that the two genes have the same expression profile and are involved in

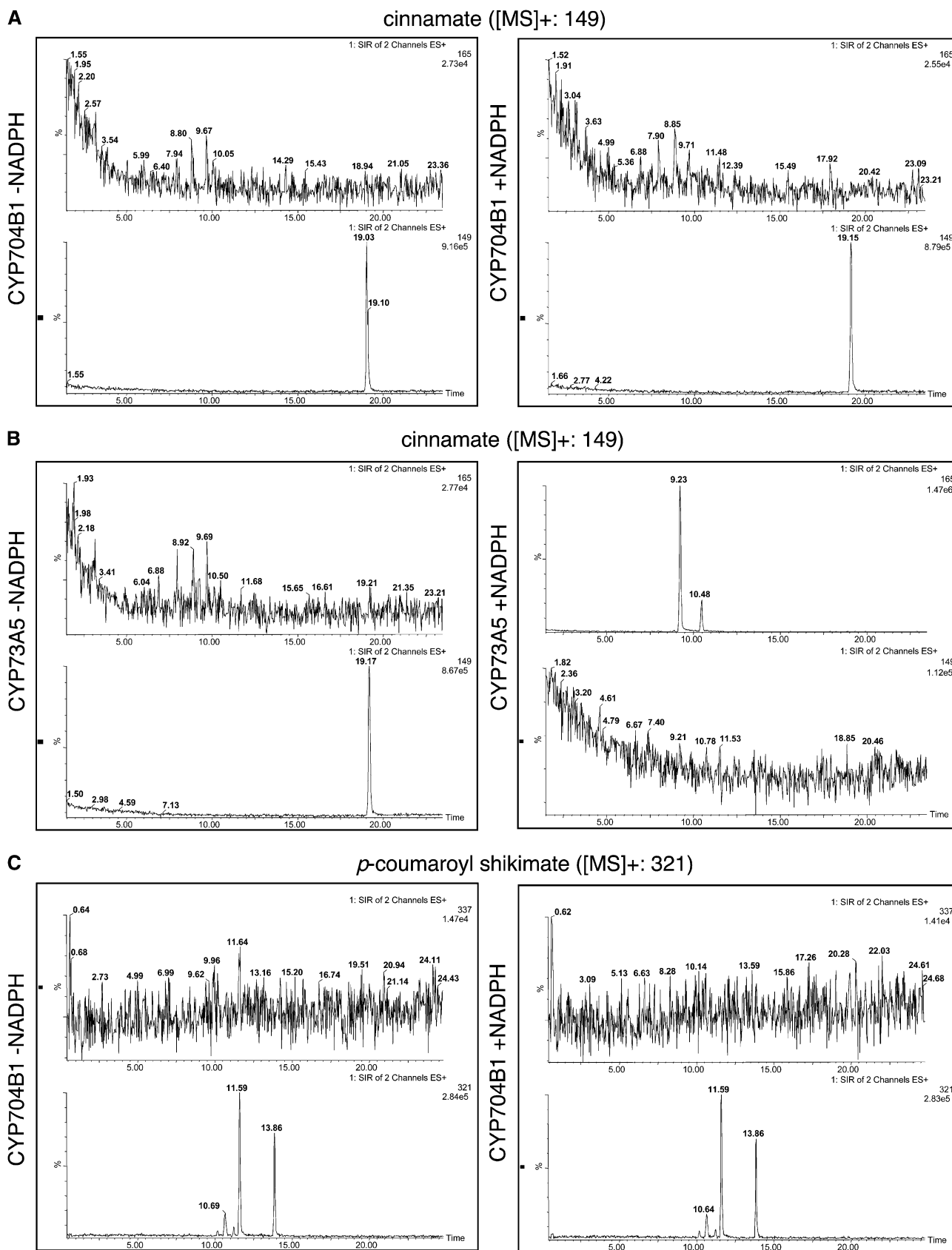


Figure 7. (Figure continues on following page.)

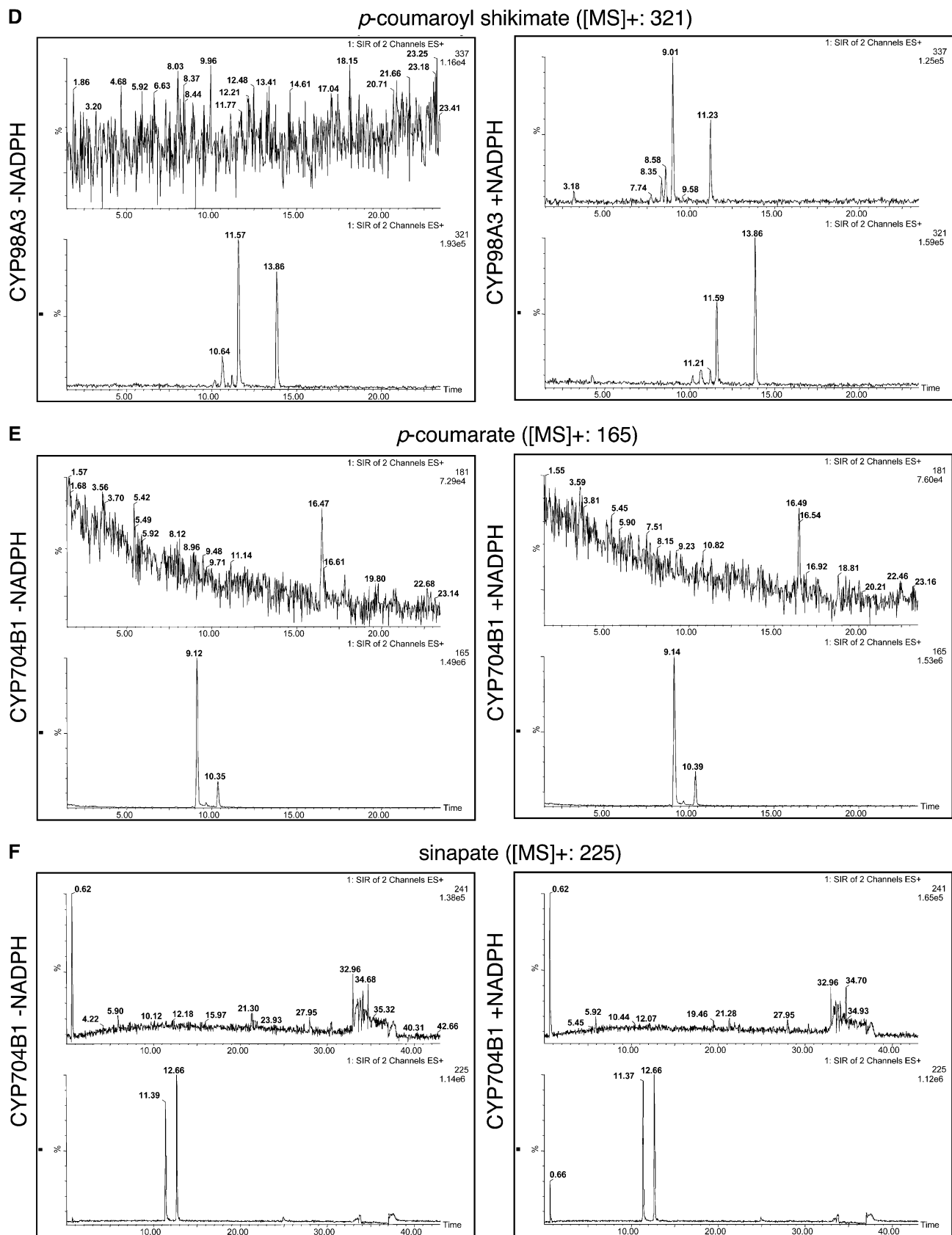
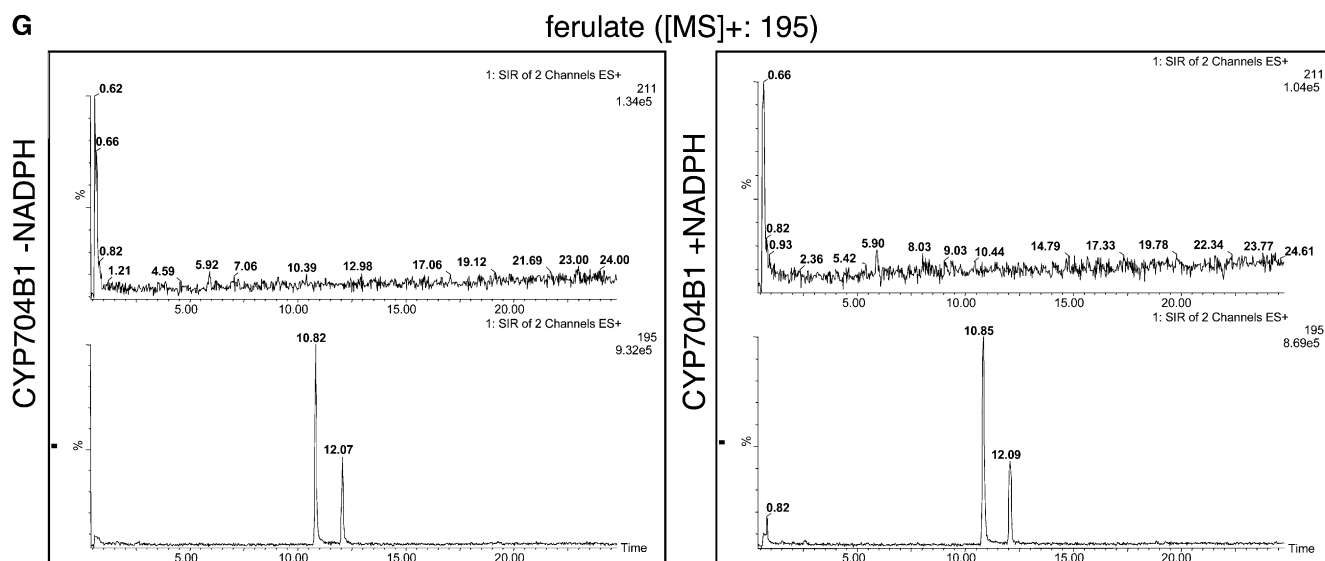


Figure 7. (Figure continues on following page.)



**Figure 7.** CYP704B1 does not hydroxylate phenolic compounds. Activities of CYP704B1-expressing microsomes toward five phenolic compounds (cinnamate [A], *p*-coumaroyl shikimate [C], *p*-coumarate [E], sinapate [F], and ferulate [G]) were measured using UPLC-MS/MS. Reactions were performed in the absence or presence of NADPH. In each panel, the top chromatogram corresponds to the predicted mass of hydroxylated product, while the bottom chromatogram corresponds to the substrate. None of the phenolic substrates was metabolized by CYP704B1. Two other CYPs (CYP73A5 and CYP98A3), known to act as hydroxylases of cinnamate and *p*-coumaroyl shikimate, respectively, served as positive controls in the reactions with the corresponding substrates (B and D).

fatty acid metabolism, we explored their relationships by creating a *cyp704b1 ms2* double mutant. T-DNA insertion alleles (SAIL\_1149\_B03 for *cyp704b1* and SAIL\_92\_C07 or SAIL\_75\_E01 for *ms2*) were used for these experiments. The F2 plants segregated the wild-type and mutant phenotypes at a ratio of 9:7 ( $\chi^2$  test;  $P = 0.2$  for crosses with SAIL\_75\_E01,  $P = 0.3$  for crosses with SAIL\_92\_C07). We genotyped the mutant plants in order to identify the double mutants. In the double mutants, we observed no reduction in the amount of pollen produced or in plant fertility ( $55 \pm 6$  seeds per silique [ $n = 10$  siliques] versus  $55 \pm 5$  seeds per silique [ $n = 10$  siliques] in the wild type). When examined by LSCM, the double mutant pollen had a *zebra* pollen surface (Fig. 8C) similar to that of the single mutants. No novel phenotypes or enhancement of single mutant phenotypes were observed in the double mutant, suggesting that *MS2* and *CYP704B1* act in the same genetic pathway required for the synthesis of the fatty acid components of sporopollenin.

#### The Pollen Surface in Null Mutants of *CYP703A2*, a Previously Described Exine Gene Encoding an In-Chain Fatty Acid Hydroxylase, Also Has *zebra* Phenotypes

The similarity of the *ms2* and *cyp704b1* mutant phenotypes prompted us to carefully examine exine phenotypes of mutants defective in *CYP703A2*, the third anther-specific gene involved in exine development and fatty acid metabolism. We found that hypomorphic alleles caused by point mutations *lap4-1* (Ile-391 → Ser substitution) and *40-4-1* (Gly-405 → Arg

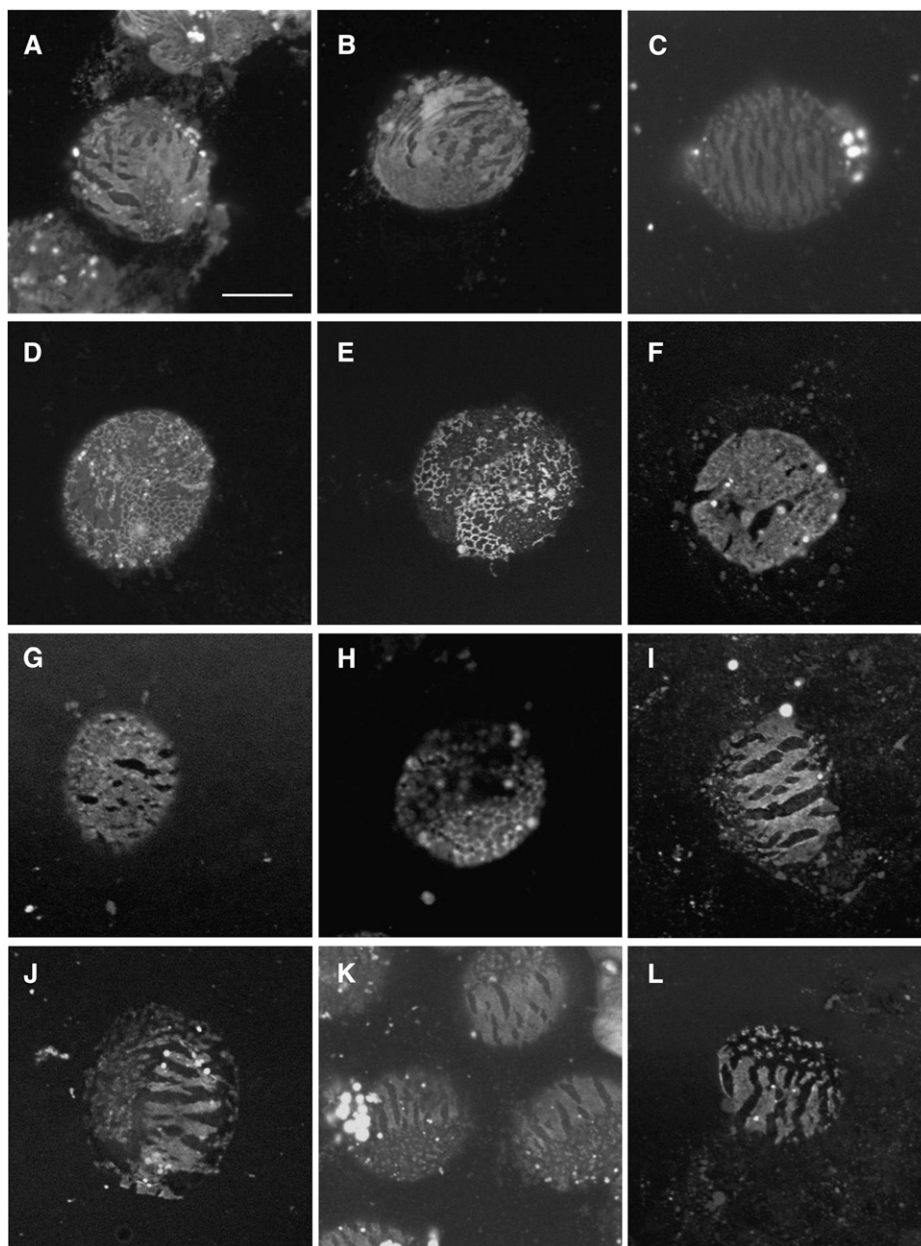
substitution; A.A. Dobritsa, unpublished data) resulted in an exine that retained the overall reticulate pattern yet was unusually thin. In addition to this, the pollen surface of these mutants often had bare patches that entirely lacked exine (Fig. 8, D and E). However, two null alleles (Morant et al., 2007) produced a *zebra*-like pollen surface with characteristic dark stripes (Fig. 8F). Exine phenotypes of these lines were somewhat variable, with most of the pollen grains exhibiting *zebra* features but some of the grains retaining remnants of the reticulate exine structures (Fig. 8H). Yet even the latter pollen grains usually had distinct *zebra* characteristics on portions of their surfaces. Double mutant combinations of *cyp703a2* (alleles *lap4-1*, SALK\_119582, and SLAT N56842) with *ms2* (allele SAIL\_92\_C07) or *cyp704b1* (allele SAIL\_1149\_B03), as well as triple *cyp703a2 cyp704b1 ms2* mutants, resulted in fertile plants that, similar to the single mutants, generated pollen with *zebra* phenotypes (Fig. 8, I–L; data not shown), suggesting that this phenotype arises whenever the fatty acid pathway in the sporopollenin synthesis is compromised.

## DISCUSSION

### CYP704B1 Acts as a Fatty Acid $\omega$ -Hydroxylase Involved in Exine Production Along with CYP703A2 and MS2

We have identified *CYP704B1* as a gene involved in the production of pollen exine. The *in vitro* functional analysis of *CYP704B1* suggests that the role of this protein is to produce long chain  $\omega$ -hydroxylated fatty

**Figure 8.** Pollen surfaces in the novel *ms2* alleles, null alleles of *cyp703a2*, and the double and triple mutant combinations of *cyp703a2*, *ms2*, and *cyp704b1* all show *zebra* phenotypes. Confocal images of auramine O-stained exine surfaces of pollen grains of the following genotypes: *ms2* T-DNA insertion alleles SAIL\_92\_C07 (A) and SAIL\_75\_E01 (B), *cyp704b1 ms2* double mutant (C), *cyp703a2* point mutants *lap4-1* (D) and 40-4-1 (E), *cyp703a2* T-DNA insertion alleles SALK\_119582 (F) and SLAT N56842 (G and H), *cyp703a2 cyp704b1* double mutant (I), *cyp703a2 ms2* double mutant (J), and *cyp703a2 cyp704b1 ms2* triple mutant (K and L). In K, the *cyp703a2* allele has a point mutation, *lap4-1*, and in L, the *cyp703a2* allele is the insertion line SALK\_119582. Point mutants of *cyp703a2* retained a reticulate exine pattern (D and E); however, their exine was very thin, and bare exineless patches were often present. Insertion mutants of *cyp703a2* sometimes had remnants of reticulate structure on portions of the grains (visible in H). Bar = 10  $\mu$ m.



acids that may serve as building blocks in sporopollenin. Although this conclusion needs to be confirmed by chemical analysis of the pollen, CYP704B1 joins CYP703A2 and MS2 as a protein implicated in exine-specific fatty acid metabolism. Investigation of co-expression patterns using ATTED-II and BAR Expression Angler identified all three genes as being highly coregulated partners. CYP704B1 catalyzes end-of-chain hydroxylation of C14-C18 fatty acids in vitro, whereas CYP703A2 encodes an in-chain hydroxylase of lauric acid (Morant et al., 2007). MS2 shares sequence homology with fatty acyl reductases (Aarts et al., 1997) and catalyzes the conversion of fatty acids to fatty alcohols when expressed in *Escherichia coli* (Doan et al., 2009). The finding that CYP703A2 acts on

lauric acid and CYP704B1 metabolizes longer fatty acids suggests that at least two types of differentially hydroxylated fatty acids may serve as monomeric building blocks during the formation of sporopollenin. Hydroxylated fatty acid units produced by CYP704B1 and CYP703A2 (and possibly fatty alcohols produced by MS2) and phenylpropanoids joined by ether and ester bonds may form the backbone of sporopollenin. The use of two or more types of fatty acids with different chain lengths and hydroxylated in different positions may add complexity to sporopollenin packing and provide higher level cross-linking that contributes to the remarkable strength of this biopolymer.

Null mutations in CYP704B1, CYP703A2, and MS2 result in very similar pollen phenotypes. The pollen

surface of these mutants completely lacks the exine layer. Instead, they exhibit a very thin irregular layer of an unknown material. One possibility is that this material corresponds to the remnants of the nexine, the simpler inner layer of exine. When stained with auramine O and viewed using LSCM, the pollen surface of all three mutants exhibits a characteristic striped *zebra* pattern. The double mutants *cyp703a2 cyp704b1*, *cyp704b1 ms2*, and *cyp703a2 ms2* and the triple mutants have phenotypes identical to those of single mutants, indicating that the three genes act complementarily and that the knockout of any of them abolishes the fatty acid branch in sporopollenin production, which in turn leads to the absence of the exine layer.

Interestingly, the phenotypes of the *cyp704b1*, *cyp703a2*, and *ms2* mutants are different from the phenotype of the recently described *acos5* mutant that affects a novel fatty acyl-CoA synthase. This enzyme exhibits *in vitro* preference for hydroxylated medium- to long-chain fatty acids (de Azevedo Souza et al., 2009). It was suggested that ACOS5 also likely participates in the biosynthesis of fatty acid constituents of sporopollenin by forming fatty acyl-CoA esters of polymer precursors (de Azevedo Souza et al., 2009). Under our growth conditions, the *cyp704b1*, *cyp703a2*, and *ms2* mutants lacked exine and had a *zebra* pollen surface, yet their pollen was viable and fertile. The *acos5* mutant, however, was completely male sterile and resulted in pollen that degenerated in the developing anthers upon the lack of exine synthesis (de Azevedo Souza et al., 2009; A.A. Dobritsa, unpublished data). The latter phenotype was similar to that of the mutants with possible defects in the phenylpropanoid branch of sporopollenin synthesis (the *lap5 lap6* double mutant affecting proteins with similarities to chalcone synthase; A.A. Dobritsa, unpublished data). These phenotypic differences between fatty acid branch mutants possibly indicate a more central role played by ACOS5 in the production of fatty acid components of sporopollenin in comparison with CYP704B1, CYP703A2, and MS2. An alternative hypothesis is that the ACOS5 CoA synthetase has an unidentified role in the phenylpropanoid branch. In this case, phenotypic differences in defects in two metabolic branches of sporopollenin synthesis may point to differential roles played by these two types of compounds in the formation of mature sporopollenin or its anchorage to the pollen surface. It should be noted that, unlike the three *ms2* alleles described here, the allele of *ms2* described by Aarts et al. (1993, 1997) resulted in male sterility due to the collapse of microspores during development. Likewise, the *cyp703a2* knockout lines were previously reported to have reduced fertility, mainly associated with impaired silique development at the base of the inflorescences (Morant et al., 2007). The nature of the discrepancy between the reported phenotypes of these lines remains unclear. Among possible causes are differences in growth conditions (e.g. different humidity, green-

house versus growth chambers), differences between ecotype backgrounds of the mutants (e.g. Columbia [Col] versus Landsberg *erecta* for *ms2* alleles), as well as the fact that some mutants were generated through transposon mobilization, which might have resulted in a second-site mutation. Aarts et al. (1997) also noted that the male-sterile phenotype of the *ms2* line they used was leaky and had variable expressivity.

### Evolution of the CYP704B Subfamily

Acquisition of sporopollenin, which provides structural support, protection against UV light, microbial attacks, and dehydration to spores and pollen, was one of the most important adaptations that allowed plants to colonize land. CYP704B1 is highly conserved in the terrestrial plants, with orthologs present in eudicots (e.g. snapdragon [*Antirrhinum majus*], grape [*Vitis vinifera*], poplar [*Populus trichocarpa*], pepper [*Capsicum annuum*], and columbine [*Aquilegia* species]), monocots (maize and rice [*Oryza sativa*]), gymnosperms (*G. biloba*), and even in the recently sequenced genome of the moss *Physcomitrella patens*. EST database searches revealed the conservation of its expression pattern. Similar to the Arabidopsis CYP704B1, its orthologs, even the ones from evolutionarily distant plants, demonstrate a strong tendency to be expressed in the developing flowers and male organs. For instance, the CYP704B1 ortholog in the monocot maize is specifically expressed in the developing tassels, while the one from the gymnosperm *G. biloba* is expressed in microsporophyll, a leaf-like structure that bears microsporangia. Similar to the effect of *cyp704b1* mutations, a mutation in an orthologous maize gene also affects pollen development (Albertsen et al., 2006). Taken together, these data strongly suggest that the CYP704B proteins in the terrestrial plants are dedicated to pollen development and have a conserved function, likely in the production of sporopollenin.

The phylogenetic analysis of the CYP704B subfamily revealed strong parallels with the CYP703 family, whose members are also involved in sporopollenin production. Similar to CYP703 and unlike other families in the CYP86 clan to which CYP704 belongs, the CYP704 family has undergone only one duplication event, separating the CYP704B and CYP704A subfamilies. Although the CYP704A subfamily, whose function is unknown at present, has undergone additional duplications (two sequences in Arabidopsis and six in rice), the CYP704B protein appears to be under strong selective pressure, supporting its important biological function. Similar to CYP703 proteins, there are single copies of CYP704B in the fully annotated genomes of Arabidopsis and rice (Nelson et al., 2004). Also, in agreement with the CYP703 data, the genome of the poplar *P. trichocarpa* contains a single functional CYP704B as well as a pseudogene (Nelson, 2008). The genome-wide duplication of the poplar genome that occurred after the split of the *Populus* and Arabidopsis lineages (Tuskan et al., 2006) might explain the pres-

ence of two copies of *CYP704B* in this species, one of which has eventually lost its function.

Similar to pollen of higher plants, spores in ferns and mosses have cell walls primarily composed of sporopollenin (Zetzsche and Vicari, 1931). The genome of the moss *P. patens* contains three *CYP703A* and three *CYP704B* genes (Nelson, 2006). It has been suggested that *P. patens* underwent a whole-genome duplication event about 30 to 60 million years ago, much later than the time of separation between bryophytes and higher plants (Rensing et al., 2007). This may account for the presence of several *CYP703A* and *CYP704B* paralogs in its genome. It remains to be investigated whether these genes are truly functionally redundant or if some of them gained a different function in evolution. We hypothesize that at least one of these genes is essential for proper spore wall development.

## MATERIALS AND METHODS

### Plant Material

The genetic screen that led to the isolation of the Arabidopsis (*Arabidopsis thaliana*) *zebra* pollen mutants and the 40-4-1 allele of *CYP703A2* will be described in detail elsewhere. In brief, we screened pooled T-DNA insertion lines (approximately 16,000 individual lines) derived from the SALK collection (Alonso et al., 2003) for the presence of anther or pollen morphological abnormalities (e.g. in size, shape, light reflection, or pollen release from anthers) distinguishable with standard stereomicroscopes (such as Zeiss Stemi-2000C) at 50× to 80× magnification. Neither anthers nor pollen underwent any treatment for primary screening. In addition, we also screened a collection of insertion mutants for 50 candidate exine genes. These genes were selected for their possible involvement in biochemical pathways that may contribute to sporopollenin production or for their anther-specific expression at the time of exine development. Potential mutants isolated by either approach underwent a secondary screen in which their exines were stained with auramine O and visualized with confocal microscopy.

T-DNA insertions into *CYP704B1* (SAIL\_1149\_B03) and *MS2* (SAIL\_92\_C07 and SAIL\_75\_E01) were obtained from the Arabidopsis Biological Resource Center. Genotype testing of the lines with respect to *CYP704B1* and *MS2* loci was carried out using the LB3 primer (5'-TAGCATCTGAATTCAT-AACCAATCTCGATACAC-3') in combination with the following primers: CS842280-LP (5'-CTTGACAGGATGATTGGCAC-3') and CS842280-RP (5'-CAACAACAACAACAACAACAAGG-3') for SAIL\_1149\_B03, ms2-CS804382-LP (5'-GGACAATCACTAAATGACATTAAATTG-3') and ms2-CS804382-RP (5'-GTTTATGTTACGGGAAGGGG-3') for SAIL\_92\_C07, and ms2-CS803563-LP (5'-GTTTATGTTACGGGAAGGGG-3') and ms2-CS803563-RP (5'-GCAT-TACTATGAGAAGAGACTTTGCC-3') for SAIL\_75\_E01. PCR fragments containing the T-DNA border sequences were sequenced for verification of the T-DNA insertions. The *lap4-1* allele of *CYP703A2* was recovered in a screen for genes that play a role in Arabidopsis pollen-stigma adhesion (Nishikawa et al., 2005). Lines were backcrossed with wild-type Col (or Landsberg *erecta* for *lap4-1*). Plants were grown in a greenhouse at 22°C with a 16-h-light/8-h-dark photoperiod and 30% relative humidity. Genotypes of F2 mutant progeny from crosses between *cyp704b1* and *ms2* insertion alleles were determined using the above primers. Genotype analysis of the F2 mutant progeny from crosses of *cyp703a2* mutations was done as described (Morant et al., 2007) for the alleles SALK\_119582 and SLAT\_N56842 and using a derived cleaved amplified polymorphic sequence marker for the allele *lap4-1* (primers *lap4-1280-EF1* [5'-CGAGCAACAACGATCAACGGCTACTGC-3'] and *lap4-1280-DR* [5'-CATGCCATAAATCTCCACCG-3']). *PstI* cuts the mutant allele.

### Confocal Microscopy

To visualize exine structure, pollen grains were stained with 0.001% (w/v) auramine O (first dissolved to 0.1% in 50 mM Tris-HCl, pH 7.5, and then diluted to 0.001% in 17% Suc) and examined by LSCM (Olympus Fluoview FV1000, 100× objective, fluorescein isothiocyanate settings).

### Transmission Electron Microscopy

Anthers were fixed in 2% glutaraldehyde and 4% paraformaldehyde in 0.1 M Na-cacodylate buffer (infiltrated under vacuum for 1 h at room temperature and then stored overnight at 4°C), washed with cacodylate buffer (three times for 5 min), postfixed with 1% OsO<sub>4</sub> for 2 h, and washed again with cacodylate buffer (twice for 15 min). Samples were dehydrated in an ethanol series (30% 50%, 70%, 95%, and 100%, 1:1 ethanol:acetone [v/v]) and in acetone and infiltrated with Spurr's resin (Electron Microscopy Sciences) using the following series of acetone mixes: 10% (overnight), 25%, 50% (both for 3 h), 75% (6 h), 90% (overnight), 100% (overnight), and 100% (3 h). Fresh Spurr's resin was then allowed to polymerize at 60°C overnight. Sections of 90 nm were cut, counterstained with saturated uranyl acetate and 2.5% lead citrate, and visualized using a FEI Tecnai F30 transmission electron microscope.

### SEM

Anthers were vacuum infiltrated with a solution of glutaraldehyde (2.5%) and paraformaldehyde (2%) in phosphate buffer (0.1 M, pH 7.2), dehydrated in a graded series of ethanol, transferred to a mixture of ethanol and hexamethyldisilazane at increasing concentrations of 25%, 50%, 75%, and 100%, and dried overnight. Dried anthers were mounted on specimen stubs using double-sided copper tape. The samples were coated with gold:palladium in a sputter coater and imaged using SEM. Anthers analyzed without fixation were directly mounted on specimen stubs using double-sided tape.

### Acetolysis

Pollen grains were placed on a glass slide, incubated under a coverslip in a drop of 9:1 (v/v) mixture of acetic anhydride and sulfuric acid at 70°C for 20 min, sealed with a nail polish, and observed on a Zeiss Axioskop (differential interference contrast optics, 100× objective).

### Cloning of *At1g69500* Promoter::*GUS* Fusion and Complementation Constructs

For expression analysis, genomic sequence from the end of upstream gene *At1g69490* to the transcription start site of *At1g69500* was amplified from Col genomic DNA using primers 5'-ATCGAATCCACGTCACGCGATG-TTTA-3' and 5'-ATCGGATCCCTCTTTGAATCTGAAAAATAAGTTC-3' containing restriction sites *EcoRI* and *BamHI* (underlined), respectively. The PCR product was ligated in front of the *GUS* gene into the pCAMBIA1381 vector.

For the complementation test, genomic sequence from the end of upstream gene *At1g69490* to 700 bp downstream of *At1g69500* was amplified from wild-type Col genomic DNA using the primers 5'-ATCTACCCGGTTCAT-GCTCAAGCGATGTTT-3' and 5'-ATCTACTGACAGGTGTTTCAAATCAA-GTCCAGA-3' containing the restriction sites *SmaI* and *SbfI* (underlined), respectively. The PCR products were ligated into the pCAMBIA2300 vector. Wild-type and SAIL\_1149\_B03 plants, respectively, were transformed with the promoter::*GUS* and complementation construct by the floral dip method (Clough and Bent, 1998), and transgenic plants were selected with hygromycin.

For promoter::*GUS* expression analysis, tissues were incubated in 90% acetone on ice, washed in 50 mM Na-phosphate buffer, pH 7.2, incubated in a *GUS* staining solution (Jones-Rhoades et al., 2007) at 37°C for 16 h, then subjected to an ethanol series (30% and 50% FAA [50% ethanol, 10% glacial acetic acid, and 5% formaldehyde] and 70% ethanol), mounted in 50% glycerol, and viewed on a Zeiss Axioskop (10× objective).

### RT-PCR

Total RNA was extracted with the RNeasy Plant Mini kit (Qiagen). For the *At1g69500* tissue expression study, RNA (1 μg) was reverse transcribed with the SuperScript III (Invitrogen) cDNA synthesis kit and PCR was performed with the primers 5'-CAAGTAGATATGCGAGGAATTGTTG-3' and 5'-CCAA-GCAATGCCTCAGAGCCTATG-3' using ExTaq DNA polymerase (TaKaRa). For *At1g69500* and *ms2* mutant transcription analysis, RNA was isolated from stage 9 to 10 buds. One microgram of RNA was treated with RQ1 DNase (Promega), one half of each sample was reverse transcribed with the SuperScript III cDNA synthesis kit (Invitrogen) per the manufacturer's instructions

(the other half served as a no-RT control), and PCR amplification was carried out with the following primers: At1g69500-CF (5'-CAGCAACAACCTCT-CACCTGG-3') and At1g69500-GR (5'-CATATCATCTTCTAATACTCC-3'); ms2-CF (5'-CTTATGTGAATGGACAAAGAC-3') and ms2-CR (5'-CACCA-TAGAAAGTGTATGGCTC-3').

## Heterologous Expression in Yeast

Total RNA extraction was carried out from flower buds using the Qiagen kit per the manufacturer's protocol. CYP704B1 cDNA was synthesized from 1  $\mu$ g of total RNA using SuperScript III first-strand synthesis supermix (Invitrogen) per the manufacturer's protocol. Forward primer (5'-GGAT-TAAAuAATGTCTTTGTGTTGGTTATAGCTTGTATGGTAACATC-3'; start codon is underlined; boldface corresponds to the mutagenized nucleotide that carries a silent mutation for improved expression in yeast) and reverse primer (5'-GGGTTAATATGAACGCTCGGATACAGTAACCTTCAAG-3'; underlined nucleotides encode a stop codon; boldface corresponds to the nucleotide mutagenized to change TAG into TAA, a preferred stop signal in yeast) were used. Cloning was done in a modified pYeDP60 (pYeDP60u) vector for rapid cloning strategy (Hamann and Møller, 2007). The cloned construct pYeDP60u-CYP704B1 was transformed into the yeast strain WAT11, expression was carried out according to Pompon et al. (1996), and expression levels were estimated by carbon monoxide difference spectrometry (Omura and Sato, 1964).

## Biochemical Analysis of Enzyme Activity

Microsomes expressing between 0.44 and 0.74  $\mu$ M of active cytochrome P450 (12 mg microsomal protein mL<sup>-1</sup>) were isolated and incubated with a series of commercially available radiolabeled fatty acids of different chain length (Perkin-Elmer Life Sciences). The standard assay (100  $\mu$ L) contained 20 mM Na-phosphate buffer (pH 7.4), a radiolabeled substrate (100  $\mu$ M, 54 Ci mol<sup>-1</sup>), plus a NADPH regenerating system (6.7 mM Glc-6-P and 0.4 units of Glc-6-dehydrogenase). The reaction was initiated by the addition of NADPH (to 1 mM), carried out for 20 min at 27°C, and stopped by the addition of 20  $\mu$ L of acetonitrile (containing 0.2% [v/v] acetic acid). Reaction mixtures were applied to TLC plates (Silica Gel G60 F254; 0.25 mm; Merck). For separation of hydroxylated fatty acids from the residual substrate, TLC plates were developed with a mixture of diethyl ether:light petroleum:formic acid (50:50:1, v/v/v). Experiments were performed in triplicate. The plates were scanned with a radioactivity detector (Raytest Rita Star). The silica gel area corresponding to the metabolites was scraped into counting vials, and the radioactivity was quantified by liquid scintillation counting. The radioactivity detected in the absence of NADPH was subtracted from the radioactivity detected in the presence of NADPH. For gas chromatography-MS analysis, the metabolites were eluted from the silica gel with 10 mL of diethyl ether and silylated with *N*-methyl-*N*-trifluoroacetamide. Mass spectra of the major metabolite generated during incubation of palmitic acid with microsomes expressing recombinant CYP704B1 showed ions at mass-to-charge ratio (relative intensity) 73 (97%) ((CH<sub>3</sub>)<sub>3</sub>Si<sup>+</sup>), 75 (100%) ((CH<sub>3</sub>)<sub>2</sub>Si<sup>+</sup> + O), 103 (21%) (CH<sub>2</sub>(OSi(CH<sub>3</sub>)<sub>3</sub>)), 117 (20%), 129 (19%), 147 (23%), 204 (22%), 217 (17%), 311 (30%), 385 (33%), 401 (82%) (M-15) (loss of CH<sub>3</sub> from trimethyl silyl group), 416 (1%) (M). This fragmentation pattern is identical to the pattern obtained with the authentic derivatized 16-hydroxypalmitic acid (Aldrich).

LC-MS analyses of fatty acid metabolites were performed as described (Morant et al., 2007). The mass spectra of the hydroxylated fatty acids were characterized by dominant fragments corresponding to M+23 (Na adduct) and M+45 (2 Na-H adduct). M+1 (proton adduct) fragments were observed for the two hydroxylated unsaturated fatty acids but not for hydroxylated palmitic acid. Additional fragments at M-17, M-35, and M-53 were observed for all three hydroxylated fatty acids and represent consecutive loss of three water molecules from the carboxy and hydroxy functional groups (Supplemental Fig. S4). The fragmentation patterns are in full agreement with the assignment of the products as  $\omega$ -hydroxylated fatty acids.

## Measurement of Recombinant Enzyme Activity with Phenolic Compounds

Microsomes expressing between 0.44 and 0.74  $\mu$ M of active cytochrome P450 were isolated and incubated with 100  $\mu$ M of each substrate and 1 mM NADPH in a total volume of 200  $\mu$ L of 20 mM potassium phosphate buffer (pH 7.4) at 28°C for 30 min. The reactions were terminated by addition of 20  $\mu$ L of

50% acetic acid and extracted with 500  $\mu$ L of ethyl acetate twice. The ethyl acetate layers were evaporated and kept at -80°C until analyzed by UPLC-MS/MS. Microsomes expressing CYP73A5 and CYP98A3 were used as positive controls in the reactions involving cinnamate and *p*-coumaroyl shikimate, as they serve as cinnamate-4-hydroxylase and *p*-coumaroyl-CoA 3'-hydroxylase, respectively (Urban et al., 1997; Schoch et al., 2001).

## UPLC-MS/MS Analysis

Phenolic compounds were dissolved in methanol and analyzed by UPLC-MS/MS (Acquity UPLC system; Waters) coupled to a Quattro Premier XE triple Quadrupole MS system; Waters Micromass) as described (Grienerberger et al., 2009). Column was a Waters Acquity UPLC BEH C18 column (2.1 mm  $\times$  100 mm, 1.7  $\mu$ m particle size) together with an Acquity UPLC BEH C18 precolumn (2.1 mm  $\times$  5 mm, 1.7  $\mu$ m particle size). Temperature of the column oven was 25°C, and injection volume was 3  $\mu$ L. Eluents were water containing 0.1% formic acid (A) and acetonitrile containing 0.1% formic acid (B). The flow rate was 0.45 mL min<sup>-1</sup>. Elution gradient was as follows: 3% to 20% B in 17 min, 20% to 50% B in 15 min, 50% to 100% B in 1 min, 100% B for 3 min, 100% to 3% B in 1 min, and 3% B for 6 min. UV spectra were recorded from 200 to 500 nm. The system was run by Mass-Lynx software (version 4.0). The electrospray ionization source was used in positive and negative mode with a capillary ionization voltage of 3.0 kV, radio frequency lens at 0 V, resolution (LM1, HM1, LM2, HM2) of 15, and ion energy 1 and 2 of 0.5. Source and desolvation temperatures were 135°C and 400°C. Flow rates of nitrogen for nebulizer and desolvation were 50 and 900 L h<sup>-1</sup>, respectively. Pressure of the argon collision gas was 3.0  $\times$  10<sup>-3</sup> mbar. Full-scan, selected ion recording, and daughter scan mode were used for qualitative analyses. Cone tensions were optimized at 25 V for all compounds.

The Arabidopsis Genome Initiative locus numbers for the genes analyzed in this article are as follows: At1g69500 (*CYP704B1*), At1g01280 (*CYP703A2*), and At3g11980 (*MS2*).

## Supplemental Data

The following materials are available in the online version of this article.

**Supplemental Figure S1.** Genomic copy of At1g69500 rescues the *zebra* pollen phenotype of the SAIL\_1149\_B03 mutant line.

**Supplemental Figure S2.** Meiosis and mitosis occur normally during pollen development of the At1g69500 mutants.

**Supplemental Figure S3.** Phylogenetic tree displaying the position of the CYP704B subfamily within the CYP86 clan.

**Supplemental Figure S4.** LC-MS analyses of metabolites produced by CYP704B1.

## ACKNOWLEDGMENTS

We are grateful to Aliza Shicoff and Ann Carlson for technical help and to Matthew Jones-Rhoades, Aretha Fiebig, and Jean Greenberg for critical reading of the manuscript. We acknowledge J.-E. Bassard for providing microsomes of yeast expressing CYP73A5 and Dr. D. Debayle for technical assistance with UPLC-MS/MS.

Received July 8, 2009; accepted August 18, 2009; published August 21, 2009.

## LITERATURE CITED

- Aarts MG, Dirkse WG, Stiekema WJ, Pereira A (1993) Transposon tagging of a male sterility gene in Arabidopsis. *Nature* **363**: 715-717
- Aarts MG, Hodge R, Kalantidis K, Florack D, Wilson ZA, Mulligan BJ, Stiekema WJ, Scott R, Pereira A (1997) The Arabidopsis MALE STERILITY 2 protein shares similarity with reductases in elongation/condensation complexes. *Plant J* **12**: 615-623
- Ahlers F, Thom I, Lambert J, Kuckuk R, Wiermann R (1999) <sup>1</sup>H NMR analysis of sporopollenin from *Typha angustifolia*. *Phytochemistry* **5**: 1095-1098
- Albertsen MC, Fox T, Huffmann G, Trimmell M (2006) Nucleotide sequences affecting plant male fertility and methods of using same. U.S. Patent 7,098,388 B2, Pioneer Hi-Bred International

- Alonso JM, Stepanova AN, Leisse TJ, Kim CJ, Chen H, Shinn P, Stevenson DK, Zimmerman J, Barajas P, Cheuk R, et al (2003) Genome-wide insertional mutagenesis of *Arabidopsis thaliana*. *Science* **301**: 653–657
- Ariizumi T, Hatakeyama K, Hinata K, Inatsugi R, Nishida I, Sato S, Kato T, Tabata S, Toriyama K (2004) Disruption of the novel plant protein NEF1 affects lipid accumulation in plastids of the tapetum and exine formation of pollen, resulting in male sterility in *Arabidopsis thaliana*. *Plant J* **39**: 170–181
- Ariizumi T, Hatakeyama K, Hinata K, Sato S, Kato T, Tabata S, Toriyama K (2003) A novel male-sterile mutant of *Arabidopsis thaliana*, *faceless pollen-1*, produces pollen with a smooth surface and an acetolysis-sensitive exine. *Plant Mol Biol* **53**: 107–116
- Benveniste I, Tijet N, Adas F, Philipps G, Salaün JP, Durst F (1998) CYP86A1 from *Arabidopsis thaliana* encodes a cytochrome P450-dependent fatty acid omega hydroxylase. *Biochem Biophys Res Commun* **243**: 688–693
- Benveniste I, Saito T, Wang Y, Kandel S, Huang H, Pinot F, Kahn RA, Salaün JP, Shimoji M (2006) Evolutionary relationship and substrate specificity of *Arabidopsis thaliana* fatty acid omega-hydroxylase. *Plant Sci* **170**: 326–338
- Bubert H, Lambert J, Steuernagel S, Ahlers F, Wiermann R (2002) Continuous decomposition of sporopollenin from pollen of *Typha angustifolia* L. by acidic methanolysis. *Z Naturforsch C* **57**: 1035–1041
- Clough SJ, Bent AF (1998) Floral dip: a simplified method for Agrobacterium-mediated transformation of *Arabidopsis thaliana*. *Plant J* **16**: 735–743
- Compagnon V, Diehl P, Benveniste I, Meyer D, Schaller H, Schreiber L, Franke R, Pinot F (2009) CYP86B1 is required for very long chain  $\omega$ -hydroxyacid and  $\alpha,\omega$ -dicarboxylic acid synthesis in root and seed suberin polyester. *Plant Physiol* **150**: 1831–1843
- de Azevedo Souza C, Kim SS, Koch S, Kienow L, Schneider K, McKim SM, Haughn GW, Kombrink E, Douglas CJ (2009) A novel fatty acyl-CoA synthetase is required for pollen development and sporopollenin biosynthesis in *Arabidopsis*. *Plant Cell* **21**: 507–525
- Dieterle M, Zhou YC, Schafer E, Funk M, Kretsch T (2001) EID1, an F-box protein involved in phytochrome A-specific light signaling. *Genes Dev* **15**: 939–944
- Doan TTP, Carlsson AS, Hamberg M, Bülow L, Stymne S, Olsson P (2009) Functional expression of five *Arabidopsis* fatty acyl-CoA reductase genes in *Escherichia coli*. *J Plant Physiol* **166**: 787–796
- Domínguez E, Mercado JA, Quesada MA, Heredia A (1999) Pollen sporopollenin: degradation and structural elucidation. *Sex Plant Reprod* **12**: 171–178
- Doyle JA, Hickey LJ (1976) Pollen and leaves from the mid-Cretaceous Potomac group and their bearing on early angiosperm evolution. In CB Beck, ed, *Origin and Early Evolution of Angiosperms*. Columbia University Press, New York, pp 139–206
- Duan H, Schuler M (2005) Differential expression and evolution of the *Arabidopsis* CYP86A subfamily. *Plant Physiol* **137**: 1067–1081
- Erdtman G (1960) The acetolysis method. *Sven Bot Tidskr* **54**: 561–564
- Friis EM, Pedersen KR, Crane PR (2001) Fossil evidence of water lilies (Nymphaeales) in the early Cretaceous. *Nature* **410**: 357–360
- Grienenberger E, Besseau S, Geoffroy P, Debayle D, Heintz D, Lapierre C, Pollet B, Heitz T, Legrand M (2009) A BAHD acyltransferase is expressed in the tapetum of *Arabidopsis* anthers and is involved in the synthesis of hydroxycinnamoyl spermidines. *Plant J* **58**: 246–259
- Guilford WJ, Schneider DM, Labovitz J, Opella SJ (1988) High resolution solid state  $^{13}\text{C}$  NMR spectroscopy of sporopollenins from different plant taxa. *Plant Physiol* **86**: 134–136
- Hamann T, Möller BL (2007) Improved cloning and expression of cytochrome P450s and cytochrome P450 reductase in yeast. *Protein Expr Purif* **56**: 121–127
- Höfer R, Briesen I, Beck M, Pinot F, Schreiber L, Franke R (2008) The *Arabidopsis* cytochrome P450 CYP86A1 encodes a fatty acid  $\omega$ -hydroxylase involved in suberin monomer synthesis. *J Exp Bot* **59**: 2347–2360
- Jones-Rhoades MW, Borevitz JO, Preuss D (2007) Genome-wide expression profiling of the *Arabidopsis* female gametophyte identifies families of small, secreted proteins. *PLoS Genet* **3**: 1848–1861
- Kandel S, Morant M, Benveniste I, Blee E, Werck-Reichhart D, Pinot F (2005) Cloning, functional expression, and characterization of CYP709C1, the first sub-terminal hydroxylase of long chain fatty acid in plants: induction by chemicals and methyl jasmonate. *J Biol Chem* **280**: 35881–35889
- Kandel S, Sauveplane V, Compagnon V, Franke R, Millet Y, Schreiber L, Werck-Reichhart D, Pinot F (2007) Characterization of a methyl jasmonate and wounding-responsive cytochrome P450 of *Arabidopsis thaliana* catalyzing dicarboxylic fatty acid formation in vitro. *FEBS J* **274**: 5116–5127
- Kandel S, Sauveplane V, Olry A, Diss L, Benveniste I, Pinot F (2006) Cytochrome P450-dependent fatty acid hydroxylases in plants. *Phytochem Rev* **5**: 359–372
- Kollatukudy PE (1981) Structure, biosynthesis and biodegradation of cutin and suberin. *Annu Rev Plant Physiol* **32**: 539–567
- Li Y, Beisson F, Koo AJK, Molina I, Pollard M, Ohlrogge J (2007) Identification of acyltransferases required for cutin biosynthesis and production of cutin with suberin-like monomers. *Proc Natl Acad Sci USA* **104**: 18339–18344
- Marocco K, Zhou Y, Bury E, Dieterle M, Funk M, Genschik P, Krenz M, Stolpe T, Kretsch T (2006) Functional analysis of EID1, an F-box protein involved in phytochrome A-dependent light signal transduction. *Plant J* **45**: 423–438
- Meuter-Gerhards A, Riegert S, Wiermann R (1999) Studies of sporopollenin biosynthesis in *Cucurbita maxima*. II. The involvement of aliphatic metabolism. *J Plant Physiol* **154**: 431–436
- Meyers BC, Tej SS, Vu TH, Haudenschild CD, Agrawal V, Edberg SB, Ghazal H, Decola S (2004) The use of MPSS for whole-genome transcriptional analysis in *Arabidopsis*. *Genome Res* **14**: 1641–1653
- Michelmore RW, Paran I, Kesseli RV (1991) Identification of markers linked to disease resistance genes by bulked segregant analysis: a rapid method to detect markers in specific genome regions by using segregating populations. *Proc Natl Acad Sci USA* **88**: 9828–9832
- Molina I, Ohlrogge JB, Pollard M (2008) Deposition and localization of lipid polyester in developing seeds of *Brassica napus* and *Arabidopsis thaliana*. *Plant J* **53**: 437–449
- Morant M, Bak S, Möller BL, Werck-Reichhart D (2003) Plant cytochromes P450: tools for pharmacology, plant protection and phytoremediation. *Curr Opin Biotechnol* **14**: 1–12
- Morant M, Jørgensen K, Schaller H, Pinot F, Möller BL, Werck-Reichhart D, Bak S (2007) CYP703 is an ancient cytochrome P450 in land plants catalyzing in-chain hydroxylation of lauric acid to provide building blocks for sporopollenin synthesis in pollen. *Plant Cell* **19**: 1473–1487
- Nelson DR (2006) Plant cytochrome P450s from moss to poplar. *Phytochem Rev* **5**: 193–204
- Nelson DR (2008) Cytochrome P450 homepage. <http://drnelson.utmem.edu/CytochromeP450.html> (October 25, 2008)
- Nelson DR, Schuler MA, Paquette SM, Werck-Reichhart D, Bak S (2004) Comparative genomics of rice and *Arabidopsis*: analysis of 727 cytochrome P450 genes and pseudogenes from a monocot and a dicot. *Plant Physiol* **135**: 756–772
- Nishikawa S, Zinkl GM, Swanson RJ, Maruyama D, Preuss D (2005) Callose ( $\beta$ -1,3 glucan) is essential for *Arabidopsis* pollen wall patterning, but not tube growth. *BMC Plant Biol* **5**: 22
- Obayashi T, Kinoshita K, Nakai K, Shibaoka M, Hayashi S, Saeki M, Shibata D, Saito K, Ohta H (2007) ATTED-II: a database of co-expressed genes and cis elements for identifying co-regulated gene groups in *Arabidopsis*. *Nucleic Acids Res* **35**: D863–D869
- Omura T, Sato R (1964) The carbon monoxide-binding pigment of liver microsomes. II. Solubilization, purification, and properties. *J Biol Chem* **239**: 2379–2385
- Pinot F, Benveniste I, Salaün JP, Loreau O, Noël JP, Schreiber L, Durst F (1999) Production in vitro by the cytochrome P450 CYP94A1 of major  $\text{C}_{18}$  cutin monomers and potential messengers in plant-pathogen interactions: enantioselectivity studies. *Biochem J* **342**: 27–32
- Pollard M, Beisson F, Li Y, Ohlrogge J (2008) Building lipid barriers: biosynthesis of cutin and suberin. *Trends Plant Sci* **13**: 236–246
- Pompon D, Louerat B, Bronine A, Urban P (1996) Yeast expression of animal and plant P450s in optimized redox environments. *Methods Enzymol* **272**: 51–64
- Rensing SA, Ick J, Fawcett JA, Lang D, Zimmer A, Van de Peer Y, Reski R (2007) An ancient genome duplication contributed to the abundance of metabolic genes in the moss *Physcomitrella patens*. *BMC Evol Biol* **7**: 130
- Schoch G, Goepfert S, Morant M, Hehn A, Meyer D, Ullmann P, Werck-Reichhart D (2001) CYP98A3 from *Arabidopsis thaliana* is a 3'-hydroxylase of phenolic esters, a missing link in the phenylpropanoid pathway. *J Biol Chem* **276**: 36566–36574

- Scott RJ** (1994) Pollen exine: the sporopollenin enigma and the physics of pattern. In RJ Scott, AD Stead, eds, *Molecular and Cellular Aspects of Plant Reproduction*. Cambridge University Press, Cambridge, UK, pp 49–81
- Sessions A, Burke E, Presting G, Aux G, McElver J, Patton D, Dietrich B, Ho P, Bacwaden J, Ko C, et al** (2002) A high-throughput *Arabidopsis* reverse genetics system. *Plant Cell* **14**: 2985–2994
- Shaw G, Yeadon A** (1966) Chemical studies on the constitution of some pollen and spore membranes. *J Chem Soc C* **1**: 16–22
- Shulze Osthoff K, Wiermann R** (1987) Phenols as integrated compounds of sporopollenin from *Pinus* pollen. *J Plant Physiol* **131**: 5–15
- Takeda S, Tadele Z, Hofmann I, Probst AV, Angelis KJ, Kaya H, Araki T, Mengiste T, Mittelsten Scheid O, Shibahara K, et al** (2004) BRU1, a novel link between responses to DNA damage and epigenetic gene silencing in *Arabidopsis*. *Genes Dev* **18**: 782–793
- Tijet N, Helvig C, Pinot F, Le Beaquin R, Lesot A, Durst F, Salaün JP, Benveniste I** (1998) Functional expression in yeast and characterization of a clofibrate-inducible plant cytochrome P-450 (CYP94A1) involved in cutin monomers synthesis. *Biochem J* **332**: 583–589
- Toufighi K, Brady SM, Austin R, Ly E, Provart NJ** (2005) The Botany Array Resource: e-northern, expression angling, and promoter analyses. *Plant J* **43**: 153–163
- Tuller G, Nemeč T, Hrastnik C, Daum G** (1999) Lipid composition of subcellular membranes of an FY1679-derived haploid yeast wild-type strain grown on different carbon sources. *Yeast* **15**: 1555–1564
- Tuskan GA, Difazio S, Jansson S, Bohlmann J, Grigoriev I, Hellsten U, Putnam N, Ralph S, Rombauts S, Salamov A, et al** (2006) The genome of black cottonwood, *Populus trichocarpa* (Torr. & Gray). *Science* **313**: 1596–1604
- Urban P, Mignotte C, Kazmaier M, Delorme F, Pompon D** (1997) Cloning, yeast expression, and characterization of the coupling of two distantly related *Arabidopsis thaliana* NADPH-cytochrome P450 reductases with P450 CYP73A5. *J Biol Chem* **272**: 19176–19186
- Wellisen K, Durst F, Pinot F, Benveniste I, Nettesheim K, Wisman E, Steiner-Lange S, Saedler H, Yephremov A** (2001) Functional analysis of the *LACERATA* gene of *Arabidopsis* provides evidence for different roles of fatty acid  $\omega$ -hydroxylation in development. *Proc Natl Acad Sci USA* **98**: 9694–9699
- Werck-Reichhart D, Bak S, Paquette S** (2002) Cytochromes P450. In CR Somerville, EM Meyerowitz, eds, *The Arabidopsis Book*. American Society of Plant Biologists, Rockville, MD, doi/10.1199/tab.0028, <http://www.aspb.org/publications/arabidopsis/>
- Wiermann R, Ahlers F, Schmitz-Thom I** (2001) Sporopollenin. In A Stenbüchel, M Hofrichter, eds, *Biopolymers*, Vol 1. Wiley-VCH Verlag, Weinheim, Germany, pp 209–227
- Wilwesmeier S, Wiermann R** (1995) Influence of EPTC (S-ethyl-dipropylthiocarbamate) on the composition of surface waxes and sporopollenin structure in *Zea mays*. *J Plant Physiol* **146**: 22–28
- Xiao F, Goodwin SM, Xiao Y, Sun Z, Baker D, Tang X, Jenks MA, Zhou JM** (2004) *Arabidopsis* CYP86A2 represses *Pseudomonas syringae* type III genes and is required for cuticle development. *EMBO J* **23**: 2903–2913
- Zetzsche F, Huggler K** (1928) Untersuchungen über die Membran der Sporen und Pollen. I. i. *Lycopodium clavatum* L. *Liebigs Ann Chem* **461**: 89–108
- Zetzsche F, Vicari H** (1931) Untersuchungen über die Membran der Sporen und Pollen. *Helv Chim Acta* **14**: 58–78
- Zimmermann P, Hirsch-Hoffmann M, Hennig L, Gruissem W** (2004) GENEVESTIGATOR: *Arabidopsis* microarray database and analysis toolbox. *Plant Physiol* **136**: 2621–2632